Applied Mathematical Modelling 38 (2014) 4371–4387

Contents lists available at ScienceDirect

Applied Mathematical Modelling

journal homepage: www.elsevier.com/locate/apm

Stochastic epidemic models: New behavioral indicators of the disease spreading

J.R. Artalejo [a], M.J. Lopez-Herrero [b,*]

[a] Department of Statistics and Operations Research, Faculty of Mathematics, Complutense University of Madrid, 28040 Madrid, Spain
[b] Faculty of Statistical Studies, Complutense University of Madrid, 28040 Madrid, Spain

ARTICLE INFO

Article history:
Received 28 April 2013
Received in revised form 11 November 2013
Accepted 13 February 2014
Available online 26 February 2014

Keywords:
Epidemiology
Stochastic model
Markov chain
Behavioral indicators

ABSTRACT

The purpose of this paper is to propose new indicators of the dynamics of infectious disease spread in stochastic epidemic models, including both global system-oriented descriptors (e.g. the final size measured as the number of individuals infected on a least one occasion during an outbreak) and individual-oriented descriptors (e.g. the time to reach an individual run of infections). We focus on birth-and-death models and the basic *SIR* epidemic model but the methodology remains valid for other nonlinear stochastic epidemic models. The theory is illustrated by numerical experiments which demonstrate that the proposed behavioral indicators can be applied efficiently.

1. Introduction

Epidemic models are widely used for understanding the mechanism that underlies the spread of an infectious disease. Roughly speaking, there are two main mathematical approaches: deterministic models based on differential equations and stochastic models that employ Markov chains, branching and diffusion processes. Early literature for studying epidemiological models was largely deterministic. However, when population sizes are small, it is now accepted that a stochastic model is more realistic [1]. This is the case of small communities sharing confined spaces such as intensive care units in hospitals, schools, prisons, small herds or local area networks of moderate size [2–5]. Even when the population size increases and the stochastic analysis becomes more difficult, the random nature of the disease dynamic requires to be taken into account.

One of the most important differences between deterministic and stochastic epidemic models is related to the role played by the reproduction ratio, R_0. The reproduction ratio, R_0, is probably the most important quantity in epidemiology. The classical biological interpretation presents R_0 as the expected number of secondary cases produced by one individual during the period of infectivity, when the individual is introduced into a completely susceptible population. From the deterministic perspective, it is well-known the threshold value of R_0 that establishes that an infection persists if $R_0 > 1$ (endemic equilibrium), while the model reaches the disease-free equilibrium (extinction) if $R_0 \leqslant 1$. In contrast, if we deal with a stochastic model with a finite population, the epidemic extinction is certain (with probability 1) regardless of the magnitude of R_0. However, the utility of R_0 to quantify the spread and severity of the stochastic epidemic still holds. For example, in a susceptible-infective-susceptible (SIS) stochastic epidemic the parameter region where the time to extinction is short can be identified by small values of R_0. In contrast, if R_0 is large, then the epidemic tends to persist for a very long time, so a state

* Corresponding author. Tel.: +34 913943987.
E-mail addresses: jesus_artalejo@mat.ucm.es (J.R. Artalejo), lherrero@estad.ucm.es (M.J. Lopez-Herrero).

http://dx.doi.org/10.1016/j.apm.2014.02.017
0307-904X/

of quasi-stationary equilibrium may be reached before a random fluctuation leads to the extinction of the epidemic. For further comparison between deterministic and stochastic models, we refer to the literature [1,6–8].

There is no reason to see a conflict between the two approaches. The advantage of the deterministic model lies in its generally simpler analysis. However, Andersson and Britton [1] conclude that stochastic models are to be preferred when their analysis is possible. To this end, the stochastic model so often contains several simplifying assumptions (e.g. exponentiality, homogeneity, randomly-mixing), and thus it is not entirely realistic. A compromise between mathematical tractability and realistic assumptions is always a premise.

In the present work, we are concerned with stochastic epidemic models that employ continuous time Markov chains (*CTMC*). More concretely, we describe the dynamics of the epidemic in terms of birth-and-death processes and the susceptible-infective-removed (*SIR*) stochastic model. Despite of the limitations assumed, this framework allows a detailed mathematical elaboration. We compute not only the expected value of the epidemic descriptors, but also their whole probability distribution (i.e., density function or probability mass function). Moreover, our mathematical results are well suited for numerical implementation. We show how algebraic computations of the epidemic indicators can be reduced to deal with iterative stable schemes.

Among the classical indicators of the spread, severity and persistence of the infectious disease, we mention the final size of the epidemic, the time to extinction and the quasi-stationary distribution [1,6–9]. The goal of this paper is to make progress by investigating other indicators of interest related both to global system-oriented characteristics and to individual-oriented descriptors of the infectious disease. Most of the indicators studied in the sequel are completely new, except the number of infections per individual which was considered in [5].

More specifically, in the case of epidemic models of birth-and-death type, we consider the following descriptors: (i) the time to reach an individual run of infections, (ii) the final size, and (iii) the number of infections per individual; while in the case of the stochastic *SIR* model the attention is focused in: (iv) the time to reach a specific state, and (v) the time to reach a critical number of infections.

In order to complete the description of the literature, we now mention a selection of related epidemiological stochastic models based on *CTMCs* [4,5,10–15], some recent papers investigating indicators of the transmissibility in *SIS* and *SIR* stochastic models [16,17], as well as some works of the authors where the main epidemic indicators were revisited [2,3,18].

The dimensionality of the underlying *CTMC* determines the order of presentation of the results, so we start presenting our findings for the unidimensional birth-and-death processes (Section 2) and the *SIS* stochastic epidemic, which is subsumed under the birth-and-death formalism as a special case. However, we remark that the bidimensional *SIR* model (Section 3) has a simpler algebraic structure, which makes the technical calculations easier. Theoretical results in Sections 2 and 3 provide the paper contribution to the development of a methodology. Our numerical results and discussion on their implications are presented in Section 4. Along the numerical experiments we perform a sensitivity analysis to determine how the system parameters will impact the new indicators. Finally, concluding remarks are given in Section 5.

2. Birth-and-death processes

We consider a closed population of size N, where each individual is classified as either a susceptible or an infective. Let $S(t)$ and $I(t)$ be the number of susceptibles and infectives, respectively, at time t. Since $S(t)+I(t)=N$, the evolution of the epidemic is simply described by the process $\{I(t); t \geqslant 0\}$ with state space $S=\{0,\ldots,N\}$. The infection ends when $I(t)=0$. The birth rates, corresponding to infections, are denoted by $\lambda_i>0$, for $1 \leqslant i \leqslant N-1$, ($\lambda_0=\lambda_N=0$) and the death rates, corresponding to recoveries, are denoted by $\mu_i>0$, for $1 \leqslant i \leqslant N$, ($\mu_0=0$). The transitions among states are represented in Fig. 1. A selected sample of epidemiological stochastic models obtained as particular cases of the birth-and-death formalism includes the basic *SIS* epidemic model, the *SIS* model with external source of infection and the Verhulst model.

The *SIS* model assumes that a recovered individual does not acquire immunity but immediately becomes susceptible. Thus, the process $\{I(t); t \geqslant 0\}$ is usually modelled as a particular case of a birth-and-death process with an absorbing state 0. The birth and death rates are

$$\lambda_i = \frac{\beta}{N} i(N-i), \quad 0 \leqslant i \leqslant N,$$
$$\mu_i = \gamma i, \quad 0 \leqslant i \leqslant N,$$

where β is the contact rate and γ is the individual recovery rate.

In the model with a external source of infection the birth rate should be modified as $\lambda_i=(\xi+\beta i/N)(N-i)$, for $0 \leqslant i \leqslant N$, where $\xi>0$ denotes the rate associated with the external source of infection. We notice that $\lambda_0>0$. Another generalization

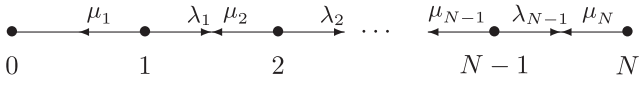

Fig. 1. States and transitions in the birth-and-death model.

is the Verhulst model with infection rates $\lambda_i = \beta i(1-(\alpha_1 i/N))$, for $0 \leqslant i \leqslant N-1$, and recovery rates $\mu_i = \gamma i(1+(\alpha_2 i/N))$, for $1 \leqslant i \leqslant N$.

There exists a vast literature focused on the study of the quasi-stationary distribution and the time to extinction in the *SIS* model and its variants [1,6,12,18–20]. The number of recovered individuals [2] observed before the extinction of the epidemic (or, alternatively, during a time interval $[0,t]$) amounts to the number of cases of infection [5]. As a result, the idea of severity of the outbreak provided by the final size [1,9,21] is extended to the context of an epidemic where immunity is not preserved.

In what follows, we investigate in detail two new epidemic descriptors, namely the time until an individual reaches a critical number of infections and the total number of individuals infected on at least one occasion during an outbreak (i.e., the final size for a non-immune model). In addition, we extend the study in Stone et al. [5] for the number of infections per individual during the outbreak.

2.1. The time to reach an individual run of infections

We mark one arbitrary individual present in the population at any arbitrary time t. Then, we introduce an extended *CTMC* $\{(K(t),I(t),N(t));t>0\}$, where $K(t)$ is equal to 0 or 1 according to whether the marked individual is susceptible or infective at time t, $I(t)$ gives the total number of infective individuals and $N(t)$ denotes the total infections suffered by the marked individual until time t. The objective is to observe the period that the marked individual will last to get $c \geqslant 1$ new recurrent infections. To this end, we extend the study conducted in Artalejo et al. [3] for the time until the first infection of a selected individual.

The extended state space, S, can be partitioned as $S = S_{A_1} \cup S_{A_2} \cup S_T$, where the set $S_{A_1} = \{(0,0,j); 0 \leqslant j \leqslant c-1\}$ contains absorbing states due to the epidemic end, the set $S_{A_2} = \{(1,i,c); 2 \leqslant i \leqslant N\}$ consists of the absorbing objective states, and the set of transient states is $S_T = \cup_{j=0}^{c-1} l(0,j) \cup \cup_{j=1}^{c-1} l(1,j)$, where the levels $l(0,j)$ and $l(1,j)$ are defined by $l(0,j) = \{(0,i,j); 1 \leqslant i \leqslant N-1\}$, for $0 \leqslant j \leqslant c-1$, and $l(1,j) = \{(1,i,j); 1 \leqslant i \leqslant N\}$, for $1 \leqslant j \leqslant c-1$. Transitions from initial states in levels $l(0,j)$, or $l(1,j)$, are represented in Figs. 2a and 2b, respectively.

For $1 \leqslant i \leqslant N-1$, rates $\widehat{\lambda}_i = \lambda_i(N-i-1)/(N-i)$ and $\widetilde{\lambda}_i = \lambda_i/(N-i)$ represent birth rates corresponding to the infection of a non marked individual or to the infection of the tagged one, respectively. Analogously, for $1 \leqslant i \leqslant N$, $\widehat{\mu}_i = \mu_i(i-1)/i$ and $\widetilde{\mu}_i = \mu_i/i$ denote the death rates associated with a recovery either of a non marked individual or of the tagged one.

Now we denote by T_{kij} the time to reach the desired run of c infections given the initial state $(k,i,j) \in S$. Notice that T_{kij} is a defective random variable because the *CTMC* can be absorbed in S_{A_1} instead in S_{A_2}. To study the random variables T_{kij}, we introduce some notation

$$\begin{aligned}
&\nu_{kij} = P\{T_{kij} < \infty\}, \quad (k,i,j) \in S,\\
&\varphi_{kij}(s) = E[e^{-sT_{kij}}\mathbf{1}_{\{T_{kij}<\infty\}}], \quad (k,i,j) \in S,\ \mathrm{Re}(s) \geqslant 0,\\
&m^n_{kij} = E[T^n_{kij}\mathbf{1}_{\{T_{kij}<\infty\}}], \quad (k,i,j) \in S,\ n \geqslant 0,
\end{aligned}$$

where, for any event A, $\mathbf{1}_A$ is the indicator random variable that takes the value 1 when the event A occurs and it is 0 otherwise.

Theorem 1 (the proof is given in Appendix A) presents a computationally stable recursive scheme for computing the Laplace transforms $\varphi_{kij}(s)$. The proposed scheme just deals with algebraic operations involving positive terms, which guarantees stability even for large population sizes. Consequently it provides, at a low computational cost, the values of the Laplace transforms and from them the density functions, $f_{T_{kij}}(x)$, can be obtained via numerical inversion methods [22,23].

Theorem 1. *The Laplace transforms $\varphi_{0ij}(s)$, for $1 \leqslant i \leqslant N-1$ and $0 \leqslant j \leqslant c-1$, and $\varphi_{1ij}(s)$, for $1 \leqslant i \leqslant N$ and $1 \leqslant j \leqslant c-1$, are computed from the equations*

$$\varphi_{0,N-1,j}(s) = \frac{\mu_{N-1}D^0_{N-2} + \lambda_{N-1}\varphi_{1Nj+1}(s)(s+g^0_{N-2}+\lambda_{N-2})}{(s+\lambda_{N-1})(s+g^0_{N-2}+\lambda_{N-2}) + \mu_{N-1}(s+g^0_{N-2}+\widetilde{\lambda}_{N-2})}, \tag{1}$$

$$\varphi_{0ij}(s) = \sum_{l=i}^{N-2}\frac{D^0_l}{\widehat{\lambda}_l}\prod_{n=i}^{l}\frac{\widehat{\lambda}_n}{s+g^0_n+\lambda_n} + \varphi_{0,N-1,j}(s)\prod_{l=i}^{N-2}\frac{\widehat{\lambda}_l}{s+g^0_l+\lambda_l}, \tag{2}$$

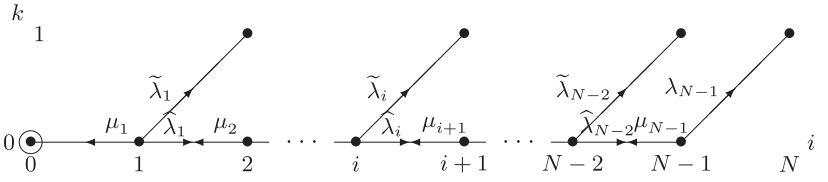

Fig. 2a. Transitions from l(0,*j*).

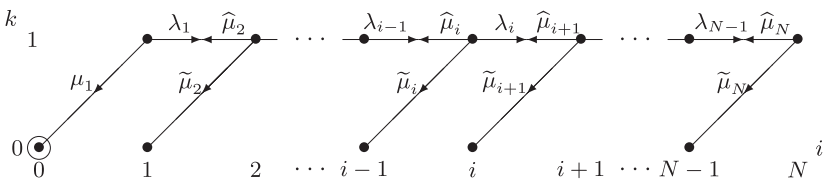

Fig. 2b. Transitions from l(1,*j*).

$$\varphi_{1Nj}(s)=\frac{\widehat{\mu}_N D^1_{N-1}+\widetilde{\mu}_N\varphi_{0,N-1,j}(s)(s+g^1_{N-1}+\lambda_{N-1})}{s(s+g^1_{N-1}+\lambda_{N-1})+\mu_N(s+g^1_{N-1})+\widetilde{\mu}_N\lambda_{N-1}}, \tag{3}$$

$$\varphi_{1ij}(s)=\sum_{l=i}^{N-1}\frac{D^1_l}{\lambda_l}\prod_{n=i}^{l}\frac{\lambda_n}{s+g^1_n+\lambda_n}+\varphi_{1Nj}(s)\prod_{l=i}^{N-1}\frac{\lambda_l}{s+g^1_l+\lambda_l}, \tag{4}$$

where the coefficients g^0_i and D^0_i, for $1\leqslant i\leqslant N-2$, are recursively determined, for each $0\leqslant j\leqslant c-1$, as follows:

$$g^0_1=\mu_1, \tag{5}$$

$$g^0_i=\mu_i\frac{s+g^0_{i-1}+\widetilde{\lambda}_{i-1}}{s+g^0_{i-1}+\lambda_{i-1}},\quad 2\leqslant i\leqslant N-2, \tag{6}$$

$$D^0_1=\widetilde{\lambda}_1\varphi_{12,j+1}(s), \tag{7}$$

$$D^0_i=\widetilde{\lambda}_i\varphi_{1,i+1,j+1}(s)+\frac{\mu_i D^0_{i-1}}{s+g^0_{i-1}+\lambda_{i-1}},\quad 2\leqslant i\leqslant N-2, \tag{8}$$

and g^1_i and D^1_i, for $1\leqslant i\leqslant N$, are determined, for each fixed $1\leqslant j\leqslant c-1$, from the recursive equations:

$$g^1_1=\mu_1, \tag{9}$$

$$g^1_i=\frac{\mu_i(s+g^1_{i-1})+\widetilde{\mu}_i\lambda_{i-1}}{s+g^1_{i-1}+\lambda_{i-1}},\quad 2\leqslant i\leqslant N-1, \tag{10}$$

$$D^1_1=0, \tag{11}$$

$$D^1_i=\widetilde{\mu}_i\varphi_{0,i-1,j}(s)+\frac{\widehat{\mu}_i D^1_{i-1}}{s+g^1_{i-1}+\lambda_{i-1}},\quad 2\leqslant i\leqslant N-1. \tag{12}$$

Moreover, for the absorbing states, we have $\varphi_{00j}(s)=0$, for $0\leqslant j\leqslant c-1$, and $\varphi_{1ic}(s)=1$, for $2\leqslant i\leqslant N$. Computation of the Laplace transforms is done under the level ordering $S_{A_1},S_{A_2},l(0,c-1),l(1,c-1),\ldots,l(0,1),l(1,1)$ and finally $l(0,0)$.

At this point, we observe that the initial density value can be determined with the help of the Tauberian result $f_{T_{kij}}(0)=\lim_{s\to\infty}s\varphi_{kij}(s)$. It yields $f_{T_{kij}}(0)=\widetilde{\lambda}_i\mathbf{1}_{A_0}$, where $A_0=\{(0,i,c-1)\in S;1\leqslant i\leqslant N-1\}$.

Note also that absorption probabilities in the set S_{A_2}, $v_{kij}=\varphi_{kij}(0)$, are null when $(k,i,j)\in S_{A_1}$, are one when $(k,i,j)\in S_{A_2}$ and, for states in S_T, they are strictly between 0 and 1. The discussion on the absorption probabilities can be completed by studying the number of infective individuals that are present in the population when the marked individual completes his *c*th infection. For a fixed i^*, with $2\leqslant i^*\leqslant N$, let us denote $f^{i^*}_{kij}$ the probability that, starting from a state $(k,i,j)\in S$, the *CTMC* is absorbed in the state $(1,i^*,c)$ (i.e., the marked individual reaches his *c*th infection and leaves behind i^* infective individuals). We observe that v_{kij} and $f^{i^*}_{kij}$ are related by $\sum_{i^*=2}^{N}f^{i^*}_{kij}=v_{kij}$, for any fixed $(k,i,j)\in S$.

For notational convenience, in what follows, we simply write f_{kij} instead of $f^{i^*}_{kij}$. Using a first-step procedure, we get that the absorbing probabilities $f^{i^*}_{kij}$ satisfy

$$f_{00j}=0,\quad 0\leqslant j\leqslant c-1,\quad f_{1ic}=0,\quad 2\leqslant i\leqslant N,\ i\neq i^*,\quad f_{1i^*c}=1,$$

$$f_{0ij}=\frac{\mu_i}{\lambda_i+\mu_i}f_{0,i-1,j}+\frac{\widehat{\lambda}_i}{\lambda_i+\mu_i}f_{0,i+1,j}+\frac{\widetilde{\lambda}_i}{\lambda_i+\mu_i}f_{1,i+1,j+1},\quad 1\leqslant i\leqslant N-1,\ 0\leqslant j\leqslant c-1, \tag{13}$$

$$f_{1ij}=\frac{\widehat{\mu}_i}{\lambda_i+\mu_i}f_{1,i-1,j}+\frac{\lambda_i}{\lambda_i+\mu_i}f_{1,i+1,j}+\frac{\widetilde{\mu}_i}{\lambda_i+\mu_i}f_{0,i-1,j},\quad 1\leqslant i\leqslant N,\ 1\leqslant j\leqslant c-1. \tag{14}$$

The coefficient matrix in the system (13) and (14) is diagonally dominant. This guarantees the existence of a unique solution, that can be achieved with the help of the forward elimination backward substitution (*FEBS*) procedure presented in Appendix A, by setting $s=0$ and f_{kij} instead of $\varphi_{kij}(s)$.

To conclude this section we deal with the moments of the time to run c recurrent infections; that is, $m^n_{kij} = (-1)^n \frac{d^n[\varphi_{kij}(s)]}{ds^n}\Big|_{s=0} = E[T^n_{kij}]$, for $(k,i,j) \in S$ and $n \geqslant 0$. Observe that $m^0_{kij} = \nu_{kij}$, for $(k,i,j) \in S$. Moreover, for $n \geqslant 1, m^n_{kij} = 0$, if $(k,i,j) \in S_{A_1} \cup S_{A_2}$.

For $n \geqslant 1$, we write Eqs. (A1) and (A2), in Appendix A, in multiplicative form. Then, we differentiate them n times, with regard to s, in order to find that

$$m^n_{0ij} = \frac{\mu_i}{\lambda_i+\mu_i} m^n_{0,i-1,j} + \frac{\widehat{\lambda}_i}{\lambda_i+\mu_i} m^n_{0,i+1,j} + \frac{\widetilde{\lambda}_i}{\lambda_i+\mu_i} m^n_{1,i+1,j+1} + \frac{n}{\lambda_i+\mu_i} m^{n-1}_{0ij}, \quad 1 \leqslant i \leqslant N-1,\ 0 \leqslant j \leqslant c-1, n \geqslant 1,$$

$$m^n_{1ij} = \frac{\widehat{\mu}_i}{\lambda_i+\mu_i} m^n_{1,i-1,j} + \frac{\lambda_i}{\lambda_i+\mu_i} m^n_{1,i+1,j} + \frac{\widetilde{\mu}_i}{\lambda_i+\mu_i} m^n_{0,i-1,j} + \frac{n}{\lambda_i+\mu_i} m^{n-1}_{1ij}, \quad 1 \leqslant i \leqslant N,\ 1 \leqslant j \leqslant c-1, n \geqslant 1.$$

This system of equations also has finite solutions due to the diagonally dominant coefficient matrix structure. In fact, the *FEBS* procedure used in the proof of Theorem 1 can be easily adapted. The following modifications are needed: (i) replace $\varphi_{kij}(s)$ by m^n_{kij}, (ii) set $s = 0$, and (iii) replace δ^0_i by $\widetilde{\lambda}_i m^n_{1,i+1,j+1} + n m^{n-1}_{0ij}$ and δ^1_i by $\widetilde{\mu}_i m^n_{0,i-1,j} + n m^{n-1}_{1ij}$.

2.2. The final size

The final size has hardly been addressed in the literature for the stochastic *SIS* epidemic model. In the paper [5] the authors make a distinction between the number of incidents of infection and the number of individuals who become infected on at least one occasion during an individual outbreak. The later descriptor was coined as *final size*. In [2], the incidence of the infectious disease was investigated through the number of recovered individuals before the extinction of the epidemic process, assuming both stationary and transient regimes. In the framework of the *SIR* epidemic model, this descriptor indeed amounts to the final size of the epidemic.

In this section, we assume that final size for the *SIS* model has the meaning expressed in [5], so that we investigate the number of different individuals that become infected during an outbreak. The re-infections of the same individual are irrelevant here. We begin by considering the bidimensional *CTMC* $\{(I(t), M(t)); t > 0\}$, where $I(t)$, as in previous section, gives the number of infective individuals in the population at time t, and $M(t)$ denotes the total number of individuals infected until time t. Let us assume that the starting state is $(I(0), M(0)) = (i_0, j_0)$, with $1 \leqslant i_0 \leqslant j_0 \leqslant N$. Then, the state space can be partitioned as $S = S_A \cup S_T$, where $S_A = \{(0,j); j_0 \leqslant j \leqslant N\}$ is the set of absorbing states, while the set of transient states is given by $S_T = \{(i,j); 1 \leqslant i \leqslant j,\ j_0 \leqslant j \leqslant N\}$.

Fig. 3 gives the state space and transitions starting from (2,2). Now rates $\widehat{\lambda}_{ij} = \lambda_i(j-i)/(N-i)$ and $\widetilde{\lambda}_{ij} = \lambda_i(N-j)/(N-i)$, for $(i,j) \in S_T$, are introduced to distinguish whether the infected individual has been infected previously or not.

For the current system state $(i,j) \in S$, we consider the random variable F_{ij} defined as the number of new individuals which are going to be infected from now until the end of the outbreak. The study of these variables consists of the analysis of their probability mass functions, generating functions, and factorial moments, which are denoted as follows:

$$x^k_{ij} = P\{F_{ij} = k\}, \quad (i,j) \in S,\ 0 \leqslant k \leqslant N-j,$$
$$\phi_{ij}(z) = E[z^{F_{ij}}], \quad (i,j) \in S,\ |z| \leqslant 1,$$
$$m^k_{ij} = E[F_{ij}(F_{ij}-1)\cdots(F_{ij}-k+1)], \quad (i,j) \in S,\ k \geqslant 1.$$

In Theorem 2 we present a recursive scheme for computing the generating functions $\phi_{ij}(z)$.

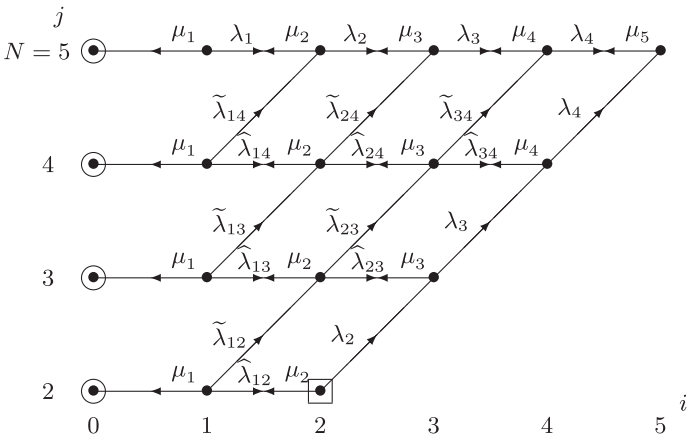

Fig. 3. The final size transitions.

Theorem 2. *For each state $j_0 \leqslant j \leqslant N$, the generating functions $\phi_{ij}(z)$ are determined from the equations*

$$\phi_{iN}(z) = 1, \quad 1 \leqslant i \leqslant N, \tag{15}$$

$$\phi_{jj}(z) = \frac{\mu_j D_{j-1} + z\lambda_j \phi_{j+1,j+1}(z)(g_{j-1} + \lambda_{j-1})}{\lambda_j(g_{j-1} + \lambda_{j-1}) + \mu_j(g_{j-1} + \widetilde{\lambda}_{j-1,j})}, \tag{16}$$

$$\phi_{ij}(z) = \sum_{k=i}^{j-1} \frac{D_k}{\widehat{\lambda}_{kj}} \prod_{n=i}^{k} \frac{\widehat{\lambda}_{nj}}{g_n + \lambda_n} + \phi_{jj}(z) \prod_{k=i}^{j-1} \frac{\widehat{\lambda}_{kj}}{g_k + \lambda_k}, \quad 1 \leqslant i \leqslant j-1, \tag{17}$$

where the coefficients g_i and D_i, for $1 \leqslant i \leqslant j-1$, are given by the recursive scheme

$$g_1 = \mu_1, \tag{18}$$

$$g_i = \mu_i \frac{g_{i-1} + \widetilde{\lambda}_{i-1,j}}{g_{i-1} + \lambda_{i-1}}, \quad 2 \leqslant i \leqslant j-1, \tag{19}$$

$$D_1 = z\widetilde{\lambda}_{1j}\phi_{2j+1}(z) + \mu_1, \tag{20}$$

$$D_i = z\widetilde{\lambda}_{ij}\phi_{i+1,j+1}(z) + \frac{\mu_i D_{i-1}}{g_{i-1} + \lambda_{i-1}}, \quad 2 \leqslant i \leqslant j-1. \tag{21}$$

Moreover, we have $\phi_{0j}(z) = 1$, for $j_0 \leqslant j \leqslant N$. Then, the computation of the generating functions is done following the reverse order $j = N, N-1, \ldots, j_0$.

Conditioning on the first transition out of the current state (i,j), we obtain

$$\phi_{ij}(z) = \frac{\mu_i}{\lambda_i + \mu_i}\phi_{i-1,j}(z) + \frac{\widehat{\lambda}_{ij}}{\lambda_i + \mu_i}\phi_{i+1,j}(z) + z\frac{\widetilde{\lambda}_{ij}}{\lambda_i + \mu_i}\phi_{i+1,j+1}(z), \quad 1 \leqslant i \leqslant j,\ j_0 \leqslant j \leqslant N. \tag{22}$$

The expressions in (15)–(17) follow along the same ideas stated on the proof of Theorem 1, so the rest of the proof is omitted.

Now we use the generating functions in order to obtain expressions for the factorial moments of F_{ij}. First we observe that the system of Eq. (22) is diagonally dominant, so it has a unique solution for $|z| \leqslant 1$. In particular, for $z = 1$, the trivial solution $\phi_{ij}(1) = 1$ gives that the order zero moments are $m_{ij}^0 = \phi_{ij}(1) = 1$, for $(i,j) \in S$.

By differentiating equations for the generating functions k times with respect to z and evaluating at $z = 1$, we find that

$$m_{0j}^k = 0, \quad j_0 \leqslant j \leqslant N,\ k \geqslant 1,$$

$$m_{ij}^k = \frac{\mu_i}{\lambda_i + \mu_i}m_{i-1,j}^k + \frac{\widehat{\lambda}_{ij}}{\lambda_i + \mu_i}m_{i+1,j}^k + \frac{\widetilde{\lambda}_{ij}}{\lambda_i + \mu_i}\left(m_{i+1,j+1}^k + km_{i+1,j+1}^{k-1}\right), \quad 1 \leqslant i \leqslant j,\ j_0 \leqslant j \leqslant N. \tag{23}$$

The above system of equation (23) also provides, after some algebra, a stable recursive scheme for computing the factorial moments of order k in terms of moments of one order less. Moreover, the recursive scheme has a similar structure as the one appearing in Theorem 2. In fact, for any integer $k \geqslant 1$, the modifications are: (i) replace $\phi_{ij}(z)$ by m_{ij}^k, (ii) set $z = 1$, and (iii) replace D_i in Eqs. (20) and (21) by $D_1 = \widetilde{\lambda}_{1j}(m_{2,j+1}^k + km_{2,j+1}^{k-1}) + \mu_1$ and $D_i = \widetilde{\lambda}_{ij}(m_{i+1,j+1}^k + km_{i+1,j+1}^{k-1}) + \mu_i D_{i-1}/(g_{i-1} + \lambda_{i-1})$, for $2 \leqslant i \leqslant j-1$, where g_i were given in Eqs. (18) and (19).

The computation of the probabilities $x_{ij}^k = P\{F_{ij} = k\}$, for $(i,j) \in S$ and $0 \leqslant k \leqslant N-j$, can be carried out by numerical inversion of $\phi_{ij}(z)$ with the help of a Fast Fourier Transform (*FFT*) algorithm [24]. As an alternative, we now propose a direct method of calculation.

When $(i,j) \in S_T$, a first-step argument gives that the probabilities satisfy

$$x_{ij}^k = \frac{\mu_i}{\lambda_i + \mu_i}x_{i-1,j}^k + \frac{\widehat{\lambda}_{ij}}{\lambda_i + \mu_i}x_{i+1,j}^k + (1 - \delta_{k0})\frac{\widetilde{\lambda}_{ij}}{\lambda_i + \mu_i}x_{i+1,j+1}^{k-1}, \tag{24}$$

where δ_{ab} stands for the Kronecker's function defined by 1, when $a = b$, and it equals 0, otherwise.

Observe that, for each fixed k, the Eq. (24) can be combined with the boundary conditions $x_{0j}^0 = 1$, for $j_0 \leqslant j \leqslant N$, in order to recursively compute the probabilities x_{ij}^k. The recursive scheme starts from $j = N$ and uses a *FEBS* procedure to determine x_{iN}^k, for $1 \leqslant i \leqslant N$, then we proceed in decreasing order with $j = N-1, \ldots, j_0$. For each fixed j, the procedure is a modification of the scheme appearing in Theorem 2 just keeping coefficients g_i as were defined in Eqs. (18) and (19), and taking D_1 equal to $\delta_{k0}\mu_1 + (1 - \delta_{k0})\widetilde{\lambda}_{1j}x_{2,j+1}^{k-1}$ and $D_i = \widetilde{\lambda}_{ij}x_{i+1,j+1}^{k-1} + \mu_i D_{i-1}/(g_{i-1} + \lambda_{i-1})$, for $2 \leqslant i \leqslant j-1$.

2.3. The number of infections per individual

As in Section 2.1, we select one of the individuals in the population who can be either an infective or a susceptible one. The objective is to study the number of subsequent infections of the marked individual during the outbreak. Stone et al. [5] investigated this random variable and, in fact, they derived matrix form expressions for the generating functions and the moments. Our purpose is twofold, first we extend the previous work by giving an alternative matrix structure which is well suited for numerical computations, and second we present a method for the direct computation of the mass distribution function avoiding the use of numerical inversion of the generating functions.

Now we pay attention to the bidimensional *CTMC* $\{(K(t), I(t)); t > 0\}$ describing both the state of the marked individual and the number of infective individuals in the population at time t. The finite state space, S, consists of a single absorbing state $(0,0)$ and the set of transient states $S_T = \{(k,i); 0 \leqslant k \leqslant 1, 1 \leqslant i \leqslant N-1+k\}$. Fig. 4 shows the state space and transitions for a population of $N = 4$ individuals, the involved parameters keep the same definitions as in Section 2.1.

By taking the number of infected individuals, $I(t) = i$, as the level of the process, we notice that the state space can be partitioned as $S = \cup_{i=0}^{N} l(i)$, where $l(0) = (0,0), l(i) = \{(0,i),(1,i)\}$, for $1 \leqslant i \leqslant N-1$, and $l(N) = (1,N)$. The generator of the Markov chain has the form

$$\mathbf{Q} = \begin{pmatrix} 0 & \mathbf{0} & \mathbf{0} & \mathbf{0} & \cdots & \mathbf{0} & \mathbf{0} & 0 \\ \mathbf{Q}_{10} & \mathbf{Q}_{11} & \mathbf{Q}_{12} & 0 & \cdots & \mathbf{0} & \mathbf{0} & \mathbf{0} \\ \mathbf{0} & \mathbf{Q}_{21} & \mathbf{Q}_{22} & \mathbf{Q}_{23} & \cdots & \mathbf{0} & \mathbf{0} & \mathbf{0} \\ \vdots & \ddots & \ddots & \ddots & \cdots & \ddots & \ddots & \\ \mathbf{0} & \mathbf{0} & \mathbf{0} & \mathbf{0} & \cdots & \mathbf{Q}_{N-1,N-2} & \mathbf{Q}_{N-1,N-1} & \mathbf{Q}_{N-1,N} \\ 0 & \mathbf{0} & \mathbf{0} & \mathbf{0} & \cdots & \mathbf{0} & \mathbf{Q}_{N,N-1} & Q_{NN} \end{pmatrix},$$

where $\mathbf{0}$ represent a block of zeroes of appropriate dimension. The description of the non zero blocks is as follows.

The blocks $\mathbf{Q}_{i,i-1}$, for $1 \leqslant i \leqslant N$, correspond to recoveries of infected individuals. On the other hand, the blocks $\mathbf{Q}_{i,i+1}$, for $1 \leqslant i \leqslant N-1$, describe the transitions due to new infections. Finally, blocks $\mathbf{Q}_{ii}$, for $1 \leqslant i \leqslant N-1$, and the scalar Q_{NN} give the rate of the exponential sojourn time in the state $(i,j) \in S_T$. In more detail, these blocks are as follows:

$$\mathbf{Q}_{10} = \begin{pmatrix} \mu_1 \\ \mu_1 \end{pmatrix}, \quad \mathbf{Q}_{i,i-1} = \begin{pmatrix} \mu_i & 0 \\ \widetilde{\mu}_i & \widehat{\mu}_i \end{pmatrix}, \quad 2 \leqslant i \leqslant N-1, \quad \mathbf{Q}_{N,N-1} = (\widetilde{\mu}_N, \widehat{\mu}_N),$$

$$\mathbf{Q}_{i,i+1} = \begin{pmatrix} \widehat{\lambda}_i & \widetilde{\lambda}_i \\ 0 & \lambda_i \end{pmatrix}, \quad 1 \leqslant i \leqslant N-2, \quad \mathbf{Q}_{N-1,N} = \begin{pmatrix} \lambda_{N-1} \\ \lambda_{N-1} \end{pmatrix},$$

$$\mathbf{Q}_{ii} = -(\lambda_i + \mu_i)\mathbf{I}_2, \quad 1 \leqslant i \leqslant N-1, \quad Q_{NN} = -\mu_N,$$

where $\mathbf{I}_2$ denotes the identity matrix.

Let us define the random variable R_{ki}, for $(k,i) \in S$, as the number of subsequent infections of the marked individual during the rest of the outbreak. In addition, we introduce some notation

$$y_{ki}^{j} = P\{R_{ki} = j\}, \quad (k,i) \in S, \ j \geqslant 0,$$
$$\psi_{ki}(z) = E[z^{R_{ki}}], \quad (k,i) \in S, \ |z| \leqslant 1,$$
$$M_{ki}^{n} = E[R_{ki}(R_{ki}-1)\cdots(R_{ki}-n+1)], \quad (k,i) \in S, \ n \geqslant 1.$$

Another appeal to first-step analysis leads to the system of equations governing the dynamics of the generating functions $\psi_{ki}(z)$. Then, the moments of order $n \geqslant 1$ are determined by appropriate differentiation. We refer the reader to the paper [5, Section 2.5 and Appendix B], where such equations were obtained. Our goal here is to exploit the block tridiagonal matrix structure of the generator $\mathbf{Q}$. In the Appendix B, we show how numerical solutions can be achieved by using a *FEBS* block algorithm and reduction of some matrices [25].

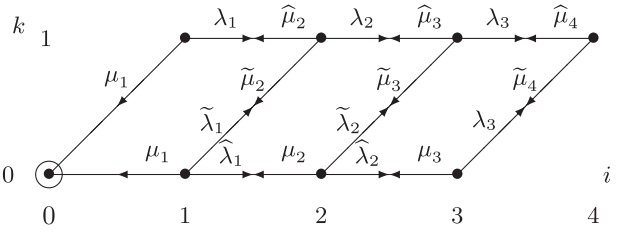

Fig. 4. The infections per individual transitions.

Next we come back to the scalar setting and propose a direct method for computing the mass function of R_{ki} as an alternative to numerical inversion procedures relying on *FFTs*. Theorem 3 provides the iterative scheme.

Theorem 3. *For each integer $j \geqslant 0$, the probabilities y_{ki}^j, with $(k,i) \in S$, are computed from the equations*

$$y_{0,N-1}^j = \frac{\mu_{N-1} D_{N-2}^0 + (1-\delta_{j0})\lambda_{N-1} y_{1N}^{j-1}(g_{N-2}^0 + \lambda_{N-2})}{\lambda_{N-1}(g_{N-2}^0 + \lambda_{N-2}) + \mu_{N-1}(g_{N-2}^0 + \widetilde{\lambda}_{N-2})},$$

$$y_{0i}^j = \sum_{k=i}^{N-2} \frac{D_k^0}{\widehat{\lambda}_k} \prod_{n=i}^{k} \frac{\widehat{\lambda}_n}{g_n^0 + \lambda_n} + y_{0,N-1}^j \prod_{k=i}^{N-2} \frac{\widehat{\lambda}_k}{g_k^0 + \lambda_k}, \quad 1 \leqslant i \leqslant N-2,$$

$$y_{1,N}^j = \frac{\widehat{\mu}_N D_{N-1}^1 + \widetilde{\mu}_N y_{0,N-1}^j (g_{N-1}^1 + \lambda_{N-1})}{\mu_N g_{N-1}^1 + \widetilde{\mu}_N \lambda_{N-1}},$$

$$y_{1i}^j = \sum_{k=i}^{N-1} \frac{D_k^1}{\lambda_k} \prod_{n=i}^{k} \frac{\lambda_n}{g_n^1 + \lambda_n} + y_{1N}^j \prod_{k=i}^{N-1} \frac{\lambda_k}{g_k^1 + \lambda_k}, \quad 1 \leqslant i \leqslant N-1,$$

where the coefficients g_i^0 and D_i^0, for $1 \leqslant i \leqslant N-2$, are determined from the following recursive scheme:

$$g_1^0 = \mu_1,$$

$$g_i^0 = \mu_i \frac{g_{i-1}^0 + \widetilde{\lambda}_{i-1}}{g_{i-1}^0 + \lambda_{i-1}}, \quad 2 \leqslant i \leqslant N-2,$$

$$D_1^0 = \delta_{j0}\mu_1 + (1-\delta_{j0})\widetilde{\lambda}_1 y_{12}^{j-1},$$

$$D_i^0 = (1-\delta_{j0})\widetilde{\lambda}_i y_{1,i+1}^{j-1} + \frac{\mu_i D_{i-1}^0}{g_{i-1}^0 + \lambda_{i-1}}, \quad 2 \leqslant i \leqslant N-2,$$

and g_i^1 and D_i^1, for $1 \leqslant i \leqslant N-1$, are recursively given by

$$g_1^1 = \mu_1,$$

$$g_i^1 = \frac{\mu_i g_{i-1}^1 + \widetilde{\mu}_i \lambda_{i-1}}{g_{i-1}^1 + \lambda_{i-1}}, \quad 2 \leqslant i \leqslant N-1,$$

$$D_1^1 = \mu_1 y_{00}^j,$$

$$D_i^1 = \widetilde{\mu}_i y_{0,i-1}^j + \frac{\widehat{\mu}_i D_{i-1}^1}{g_{i-1}^1 + \lambda_{i-1}}, \quad 2 \leqslant i \leqslant N-1.$$

Given $j \geqslant 0$, a first FEBS procedure provides the probabilities y_{0i}^j, for $1 \leqslant i \leqslant N-1$, then a second FEBS recursion gives y_{1i}^j, for $1 \leqslant i \leqslant N$.

We trivially have for the absorbing state that $y_{00}^0 = 1$. Moreover, conditioning on the first transition out of each transient state, we find that

$$y_{0i}^j = \frac{\mu_i}{\lambda_i + \mu_i} y_{0,i-1}^j + \frac{\widehat{\lambda}_i}{\lambda_i + \mu_i} y_{0,i+1}^j + (1-\delta_{j0}) \frac{\widetilde{\lambda}_i}{\lambda_i + \mu_i} y_{1,i+1}^{j-1}, \quad 1 \leqslant i \leqslant N-1,$$

$$y_{1i}^j = \frac{\widehat{\mu}_i}{\lambda_i + \mu_i} y_{1,i-1}^j + \frac{\lambda_i}{\lambda_i + \mu_i} y_{1,i+1}^j + \frac{\widetilde{\mu}_i}{\lambda_i + \mu_i} y_{0,i-1}^j, \quad 1 \leqslant i \leqslant N.$$

For each fixed $j \geqslant 0$, the recursive scheme for the computation of the probabilities y_{ki}^j is similar to that given in the proof of Theorem 1, so we omit unnecessary details here.

For any starting state (k,i), the computation can be stopped at the first integer j^* such that the cumulative mass function $\sum_{j=0}^{j^*} y_{ki}^j$ reaches a desired percentile.

3. Stochastic SIR model

In the *SIR* model, infected individuals remain infectious for a random time, but they recover and become immune. Thus, at time t, the population consists of $I(t)$ infectives, $S(t)$ susceptibles and $R(t) = N - I(t) - S(t)$ immune individuals, where N is the constant population size. We assume the initial condition $(I(0), S(0), R(0)) = (m, n, 0)$, so $N = m + n$. Thus, the population dynamics is described in terms of a bidimensional *CTMC* $\{I(t), S(t)); t \geqslant 0\}$. When in state (i,j), for $i \geqslant 1$, the population state moves either to $(i+1, j-1)$ at a rate λ_{ij}, due to an infection, or to $(i-1, j)$ at a rate μ_i, due to the removal of a infective. In the states $(i,0)$, for $1 \leqslant i \leqslant m+n$, only a removal can occur. The state space of the *SIR* epidemic model is $S = \{(i,j); 0 \leqslant j \leqslant n, 0 \leqslant i \leqslant m+n-j\}$. Since the infection ends when $I(t) = 0$, the state space can be decomposed into the set of absorbing states $S_A = \{(0,j); 0 \leqslant j \leqslant n\}$ and the set of transient states $S_T = S - S_A$. It is reasonable to assume that $m \geqslant 1$. Usually, the transition rates are assumed to be as follows

$$\lambda_{ij} = \frac{\beta}{N} ij, \quad (i,j) \in S, \tag{25}$$

$$\mu_i = \gamma i, \quad 0 \leqslant i \leqslant m+n, \tag{26}$$

where β and γ denote the contact and the recovery rates, respectively. Fig. 5 shows the state space and transitions, when $(m,n) = (3,3)$. Various authors [26,27] suggest other possibilities for the contact and removal rates including logistic, bilinear, potential and other nonlinear functions.

We notice that S_T is a reducible set. This fact influences the quasi-stationary distribution which, for the transition rates (25) and (26), gives all the probability mass to the state $(1,0)$ [18,20]. In fact, the importance of the quasi-stationary distribution depends on the type of disease being considered. For epidemic dynamics that confers immunity, the usefulness of quasi-stationarity is rather limited. Another possibility is the use of the ratio of expectations distribution [18].

A more general model assumes that infected individuals remain infectious for a general random period [1]. The bimodal nature of the final size distribution [1] and the time to extinction [3] is a remarkable feature of the *SIR* stochastic model. Bimodality can be interpreted in terms of the reproduction ratio $R_0 = \beta/\gamma$. If m is small and $R_0 \leqslant 1$, then one might expect a small epidemic so the final size and the time to extinction exhibit unimodal distributions. However, if m is small but $R_0 > 1$, then either a small or major epidemic can occur, which explains the bimodal shape of the distribution.

In the rest of this section, we give new results for the time that the epidemic needs to reach certain critical levels. More concretely, we study the time to reach a given transient state (i_0,j_0) and the time to reach a critical number of infections.

3.1. The time to reach a specific state

We are interested in the time to reach a specific state, say $(i_0,j_0) \in S$. If $(i_0,j_0) \in S_A$, then the time under study is an absorption time. Thus, it can be analyzed in a similar way as the extinction time in [3]. In contrast, if $(i_0,j_0) \in S_T$, then the time to reach (i_0,j_0) can be interpreted as a threshold state beyond what some management actions are needed in order to control the epidemic spread.

There exist two dual approaches to study the time to reach the state (i_0,j_0). The first possibility is to define the random variable T_{ij} as the time to reach the state (i_0,j_0) given that the current state is $(i,j) \in S_T$. Since the initial state is (m,n), we are specially interested in T_{mn}. However, the knowledge of T_{mn} implies to deal with a system involving the variables T_{ij} for all states $(i,j) \in S$. On the other hand, it is also possible to keep fixed the initial state (m,n) and define by L_{ij} the time to reach the state $(i,j) \in S$. We notice that $T_{mn} = L_{i_0j_0}$. In what follows, we will follow the second approach. More concretely, our algorithmic schemes for the computation of Laplace transforms and moments generalize a methodology introduced in [28] for the numerical implementation of the final size.

We are concerned with the following characteristics of the random variable L_{ij}:

$$\theta_{ij} = P\{L_{ij} < \infty\}, \quad (i,j) \in S,$$
$$\Phi_{ij}(s) = E[e^{-sL_{ij}} \mathbf{1}_{\{L_{ij}<\infty\}}], \quad (i,j) \in S, \ \mathrm{Re}(s) \geqslant 0,$$
$$\widetilde{m}_{ij}^{k} = E[L_{ij}^{k} \mathbf{1}_{\{L_{ij}<\infty\}}], \quad (i,j) \in S, \ k \geqslant 0.$$

In the *SIR* epidemic model, once a state has been visited, the system leaves it forever. This fact allows us to develop recursive schemes for the computation of the above characteristics. The algorithmic description is provided in the Appendix C.

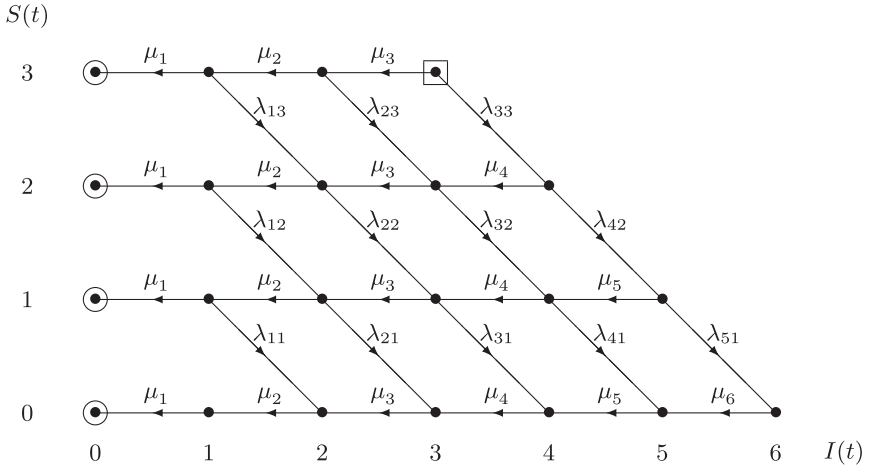

Fig. 5. States and transitions of the *SIR* epidemic model.

3.2. The time to reach a critical number of infections

In this section, we focus on the transmission potential of the infectious disease before the extinction of the epidemic. To this end, we investigate the time to reach a critical number of infections $h \geqslant 1$. This random variable amounts to the absorption time in the set $S_h = \{(i,j); 2 \leqslant i \leqslant m+h, j = n-h\}$, where $1 \leqslant h \leqslant n$. The initial objective is to study S_{mn} but it implies to deal with the absorption times S_{ij}, given that the current state is (i,j). The main difference between S_{mn} and the time to reach a specific state studied in Section 3.1 is that S_{mn} aims to measure the infection transmissibility regardless of the final number of infectives in the population.

Next we define absorption probabilities, Laplace transforms and moments of the random variable S_{ij} as follows:

$$\tau_{ij} = P\{S_{ij} < \infty\}, \quad (i,j) \in S,$$
$$\Psi_{ij}(s) = E[e^{-sS_{ij}}\mathbf{1}_{\{S_{ij}<\infty\}}], \quad (i,j) \in S,\ \mathrm{Re}(s) \geqslant 0,$$
$$\widehat{m}_{ij}^{k} = E[S_{ij}^{k}\mathbf{1}_{\{S_{ij}<\infty\}}], \quad (i,j) \in S,\ k \geqslant 0.$$

We observe that the absorption probabilities τ_{ij} are null in the set S_A, are one for $j = n-h$ and $2 \leqslant i \leqslant m+n-j$, and, for the rest of states, $\tau_{ij} \in (0,1)$. In the Appendix D we provide recursive schemes, involving just positive terms, for computing the above characteristics.

We stress again that the computation of the Laplace transforms is the key to invert numerically the density functions $f_{S_{ij}}(x)$. From the Tauberian result, we determine that $f_{S_{ij}}(0) = \lim_{s\to\infty} s\Psi_{ij}(s) = \lambda_{ij}\mathbf{1}_{A_h}$, where $A_h = \{(i, n-h+1); 1 \leqslant i \leqslant m+h-1\}$. In addition, the use of numerical inversion algorithms permits us to compute $P\{S_{mn} \leqslant x\}$; that is, the probability that, starting from the state (m,n), the time to reach h new infections takes no more than x units time.

To conclude this section we observe the following relationships between the characteristics of the random variables S_{ij} and L_{ij}:

$$\tau_{mn} = 1 - \sum_{j=n-h+1}^{n} \theta_{0j},$$
$$\Psi_{mn}(s) = \sum_{i=1}^{m+h-1} \frac{\lambda_{i,n-h+1}}{s + \lambda_{i,n-h+1} + \mu_i}\Phi_{i,n-h+1}(s),$$
$$\widehat{m}_{mn}^{k} = \sum_{i=1}^{m+h-1} \frac{\lambda_{i,n-h+1}}{\lambda_{i,n-h+1} + \mu_i} \sum_{p=0}^{k} \binom{k}{p} \widetilde{m}_{i,n-h+1}^{p} \frac{(k-p)!}{(\lambda_{i,n-h+1} + \mu_i)^{k-p}}, \quad k \geqslant 0.$$

4. Numerical results

In this section, we present some numerical illustrations of our theoretical findings. The underlying epidemic model is the stochastic *SIS* model with an external source of infection described in Section 2. For the descriptors studied in previous sections, in Sections 4.1 and 4.2, we investigate the influence of various system parameters in the behavior characteristics of the *SIS* and *SIR* epidemic models.

4.1. Behavioral analysis of the SIS epidemic model

In this section, we deal with an *SIS* epidemic model with $N = 100$ and $\gamma = 1.0$. First, we present results regarding the computation of the density function and the moments of the time to reach an individual run of $c = 3$ infections. In Table 1, we report the absorbing probability, v_{kij}, the normalized expected value, m_{kij}^{*}, and the normalized standard deviation, σ_{kij}^{*}, for $k = 0$ (i.e., the marked individual is at the susceptible state) and the combinations of $\beta = 0.75, 0.9, 1.0, 1.25, 1.75, i = 1, 50, 99$ (current number of infectives) and $j = 0, 2$ (number of previous infections suffered by the marked individual).

For a fixed pair (i,j), if we increase the number of infectives i, then we observe that v_{0ij} increases, while m_{0ij}^{*} and σ_{0ij}^{*} decrease. This behavior shows that the risk of acquiring an individual run of infections becomes higher as far as the proportion of infected individuals grows in the population. With respect to the number of infections suffered by the tagged individual, we obtain that $v_{0i0} < v_{0i2}, m_{0i0}^{*} > m_{0i2}^{*}$ and $\sigma_{0i0}^{*} > \sigma_{0i2}^{*}$. In agreement with the expectations, these results show that an individual with a past of two infections is more exposed to a new case than an individual with a virgin epidemiological history. Despite this obvious fact, the absorbing probabilities and the moments provide a good measure of the degree of exposition of an individual given that his number of previous infections is known. Finally, we also comment on the influence of the contact rate. The absorbing probabilities increase as far as the rate β is faster. On the other hand, both m_{0ij}^{*} and σ_{0ij}^{*} have a maximum, when they are considered functions of β. The existence of this peak is probably related to the underlying nonlinear form of the logistic transmission rates λ_i. In fact, the logistic function has also a peak at the point $N/2$.

In Fig. 6, for the case $j = 2$, we display the normalized density functions $f_{T_{0i2}}^{*}(x) = f_{T_{0i2}}(x)/v_{0i2}$ corresponding to the contact rate $\beta = 1.25$ and the initial states $i = 1, 50, 99$. The numerical inversion confirms that the initial value $f_{T_{0i2}}^{*}(0) = \beta i/N v_{0i2}$ is in

Table 1
Performance characteristics of $T_{0ij}: v_{0ij}, m^*_{0ij}$ and σ^*_{0ij}, versus $(0,i,j)$ and β.

	$(0,1,0)$	$(0,50,0)$	$(0,99,0)$	$(0,1,2)$	$(0,50,2)$	$(0,99,2)$
$\beta = 0.75$	0.00016	0.03414	0.07666	0.02454	0.56696	0.72427
	11.76843	7.18912	6.36935	3.12215	2.12528	1.65933
	5.40538	4.30571	4.00317	3.05793	2.53858	2.22789
$\beta = 0.90$	0.00193	0.13032	0.21664	0.04613	0.73466	0.84989
	15.64612	9.66115	8.38741	4.50902	2.59361	1.89231
	7.32594	6.09302	5.64706	4.28626	3.31152	2.79955
$\beta = 1.0$	0.00942	0.29030	0.39929	0.07262	0.84218	0.91809
	18.47089	11.55123	9.94239	5.71154	2.87465	2.00609
	8.73758	7.46477	6.92949	5.24046	3.83241	3.15681
$\beta = 1.25$	0.13742	0.88915	0.92178	0.19596	0.98762	0.99498
	19.32501	11.78476	10.13167	7.29608	2.55660	1.67703
	8.71781	7.42050	6.90715	5.73165	3.44547	5.69580
$\beta = 1.75$	0.41380	0.99999	0.99999	0.42279	0.99999	0.99999
	10.24807	6.05071	5.46218	4.68964	1.27349	0.87110
	3.50137	2.85042	2.75509	2.72604	1.35901	1.10341

agreement with the Tauberian result given in Section 2.1. The densities plotted in the figure are decreasing functions for $i = 50, 99$, while the density for $i = 1$ has a peak around 3.6. The flat shape of $f^*_{T_{012}}(x)$ agrees with the fact that the expected value m^*_{012} becomes larger as far as the initial number of infectives decreases.

For the sake of completeness, in Fig. 7 we consider the case where the marked individual has not been previously infected. Then, the Tauberian result for the case $j = 0$ says that the initial value of the density functions is $f^*_{T_{0i0}}(0) = 0$. As a result, the three curves have an unimodal shape. The tail behavior is in correspondence with the obtained expectations m^*_{0i0}, so that the tail of the distribution becomes heavier as far as i decreases. In fact, the expected value 10.13167 associated with $i = 99$ almost halves the corresponding expectation 19.32501 for $i = 1$.

In Table 2, we summarize some important characteristics of the number of infections per individual R_{ki}. We again assume that $N = 100$ and $\gamma = 1.0$. For $\beta = 0.75, 1.0, 1.25, k = 0, 1$ and $i = 1 + k, 50 + k, 99 + k$, we present from top to bottom the following quantities: the expected value, M^1_{ki}, the $99th$ percentile, j_{99}, and the mode, R^m_{ki} (i.e., the value j with highest probability mass y^j_{ki}).

From the table, it is inferred that the three characteristics are increasing functions of the initial number of infectives, i, and the contact rate, β. The values of j_{99}, and R^m_{ki} show that the distribution of the random variable R_{ki} becomes more dispersed as far as i and/or β increase. Then, the possibility of having multiple instances of infection is more likely than to have few or none. On the other hand, no significant differences are observed when the initial state k of the marked individual is varied.

4.2. Behavioral analysis of the SIR epidemic model

In this numerical experiment, we are concerned with the time to reach a critical number of infections in an *SIR* epidemic model with $N = m + n = 30$ and $\gamma = 1.0$. For the case $(m,n) = (1,29)$, in Table 3, we collect, from top to bottom, the probability of reaching at least h infections during the outbreak, τ_{mn}, the normalized expected value of S_{mn} (i.e., $m^*_{mn} = \widehat{m}^1_{mn}/\tau_{mn}$) and the normalized standard deviation (i.e., $\sigma^*_{mn} = (\widehat{m}^2_{mn}/\tau_{mn} - (m^*_{mn})^2)^{1/2}$). The critical number of infections varies as $h = 1, 8, 15, 22, 29$, while the contact rate takes the values $\beta = 0.05, 0.5, 1.0, 5.0, 10.0$.

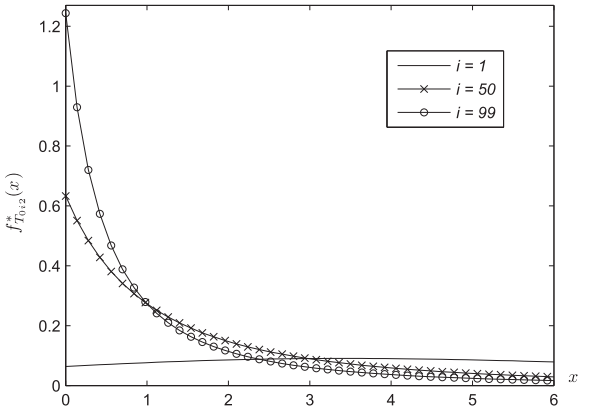

Fig. 6. Density functions $f^*_{T_{0i2}}(x)$, when $\beta = 1.25$.

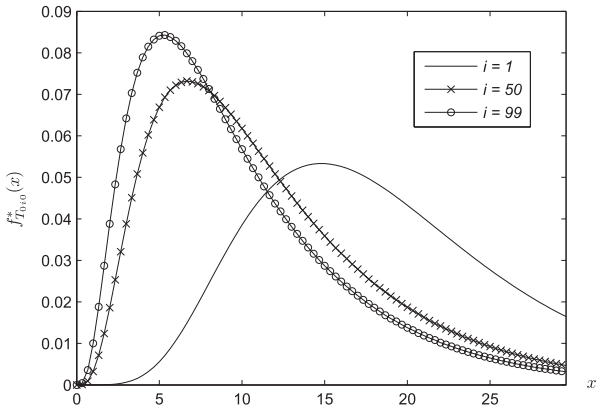

Fig. 7. Density functions $f^*_{T_{0i0}}(x)$, when $\beta = 1.25$.

Table 2
Performance characteristics of $R_{ki} : M^1_{ki}, j_{99}$ and mode, versus (k,i) and β.

	$(0,1)$	$(0,50)$	$(0,99)$	$(1,2)$	$(1,51)$	$(1,100)$
$\beta = 0.75$	0.02638	0.77811	1.11398	0.03483	0.57691	0.79632
	1	3	4	1	3	3
	0	0	1	0	0	0
$\beta = 1.0$	0.11228	1.93423	2.37651	0.18869	1.66684	1.97898
	2	7	7	3	1	7
	0	1	2	0	0	1
$\beta = 1.25$	1.98627	12.76425	13.32181	3.54086	12.43726	12.85728
	33	54	55	39	54	54
	0	3	4	0	3	4

If we fix β, then we observe that τ_{mn} decreases for increasing values of h, while m^*_{mn} and σ^*_{mn} are increasing functions of h. On the other hand, for a fixed h, we notice that τ_{mn} is increasing with β, but m^*_{mn} and σ^*_{mn} are decreasing functions of the contact rate. If at least one infection takes place, then $S_{1,29}$ is exponentially distributed with rate $\lambda_{1,29} + \beta_1$. This explains that $m^*_{1,29} = \sigma^*_{1,29} = (\lambda_{1,29} + \beta_1)^{-1}$. Regardless of the monotonicity observations, we remark that it is important to measure both the risk and the speed at which the subsequent episodes occur. For example, if $\beta = 5.0$, provided that the whole population becomes infected (i.e., the level $h = 29$ is reached), then the invasion occurs in 2.40641 (average) time units.

In Fig. 8, the epidemic is assumed to stay at different states $(i,j) = (1,29), (2,28), (3,27)$. Then, the density function of the absorption time in the set S_3 (i.e., we take $h = 3$) is plotted for the case $\beta = 1.25$ and $\gamma = 1.0$. Normalized densities associated with the pairs $(1,29)$ and $(2,28)$ have a peak, while the density corresponding to the initial state $(3,27)$ decreases from its initial value $f^*_{S_{3,27}}(0) = \lambda_{3,27}/\tau_{3,27} = 3.76763$. Thus, the curves corroborate the information provided by the Tauberian result. We notice that $m^*_{1,29} = 1.15080, m^*_{2,28} = 0.69797$ and $m^*_{3,27} = 0.31468$. These values reflect that the expected time to reach $h = 3$ infections decreases as far as the current number of infectives increases.

Table 3
Performance characteristics of $S_{1,29} : \tau_{1,29}, m^*_{1,29}$ and $\sigma^*_{1,29}$, versus h and β.

	$h = 1$	$h = 8$	$h = 15$	$h = 22$	$h = 29$
$\beta = 0.05$	0.04610	8.4×10^{-9}	8.1×10^{-16}	3.8×10^{-24}	7.1×10^{-36}
	0.95389	6.08556	9.52669	12.30168	14.69483
	0.95389	2.45691	3.21182	3.80429	4.31417
$\beta = 0.5$	0.32583	0.01457	0.00064	4.6×10^{-6}	5.5×10^{-11}
	0.67415	4.06927	6.63138	8.93123	11.05968
	0.67415	1.75089	2.39181	2.93397	3.42223
$\beta = 1.0$	0.49152	0.14578	0.05410	0.00757	7.2×10^{-6}
	0.50847	2.83817	4.70461	6.60627	8.56266
	0.50847	1.28975	1.82561	2.32563	2.78193
$\beta = 5.0$	0.82857	0.78826	0.78758	0.78685	0.59223
	0.17142	0.64969	0.92261	1.24228	2.40641
	0.17142	0.30686	0.36163	0.43660	0.97841
$\beta = 10.0$	0.90625	0.89557	0.89557	0.89557	0.88976
	0.09375	0.31495	0.42986	0.55446	0.99543
	0.09375	0.14334	0.15595	0.16963	0.36737

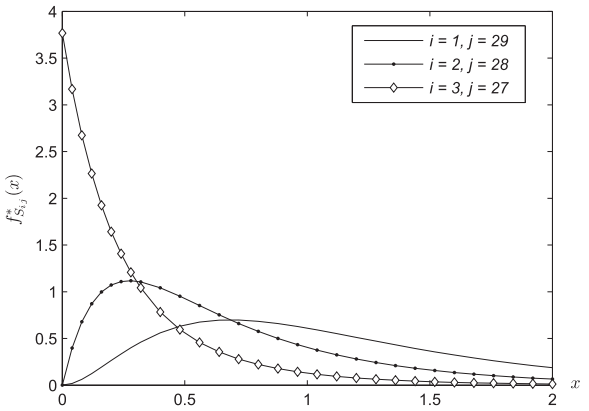

Fig. 8. Density functions $f^*_{S_{ij}}(x)$, when $(h,\beta) = (3, 1.25)$.

5. Conclusions

We have developed new indicators of the disease spreading including global system-oriented descriptors and individual-oriented ones. From the mathematical analysis of these new indicators, we gain epidemiological insight specially regarding aspects like the recurrence of the epidemic episodes. To this end, we study both continuous descriptors (e.g. time to reach an individual run of infections) and discrete descriptors (e.g. number of infections per individual).

In a more general setting, our findings aim to provide a starting point for examining the dynamics of other real epidemiological applications. In this sense, we mention those infectious diseases where the recurrence plays a significant role such as head lice infections [5], the recurrent exacerbations of chronic obstructive pulmonary disease (COPD) [29] and the recurrent urinary tract infection (UTI) [30]. Since 1990 the prevalence of head lice infections is increasing and in some situations head lice infestation seems to persist indefinitely; this may be due to various causes, resistance to insecticidal treatment has been evidenced by clinical trials but also re-infestation should be taken into account. A COPD patient should have at least two episodes of acute exacerbations in one year to be considered a candidate to change the guidelines based treatment. In the case of UTIs, a recurrent infection refers to at least two infections in six months or more than three infections in one year. In such a case, a longer course antibiotic therapy may be needed instead of a simple patient-initiated microbial therapy.

An application to outbreaks of head lice in UK schools will appear as a companion paper of this theoretical work. To this end, we have assumed the maximum likelihood estimates provided by Stone et al. [5] for fitting an *SIS* model to the head lice data. The reader interested in methods of estimation from epidemiological data is referred to [1,31,32] and the references therein.

The study can be continued in other directions. For example, it would be interesting to explore the application of our behavioral indicators to epidemics operating under an external environment including periodic seasonal patterns and switching [33–35]. We leave this possibility for a possible future study.

Acknowledgement

The authors are grateful for the helpful comments and suggestions of the reviewers and editors. This work was supported by the Government of Spain (Ministry of Science and Innovation) and the European Commission through project MTM 2011-23864.

Appendix A. Proof of Theorem 1

A first-step argument, conditioning on the identity of the next involved individual and also on the observed event (i.e., an infection or recovery of a non tagged individual, the infection or recovery of the marked individual), gives that Laplace transforms, $\varphi_{kij}(s)$, satisfy the following set of equations:

$$\varphi_{0ij}(s) = \frac{\mu_i}{s+\lambda_i+\mu_i}\varphi_{0,i-1,j}(s) + \frac{\widehat{\lambda}_i}{s+\lambda_i+\mu_i}\varphi_{0,i+1,j}(s) + \frac{\widetilde{\lambda}_i}{s+\lambda_i+\mu_i}\varphi_{1,i+1,j+1}(s), 1 \leqslant i \leqslant N-1, 0 \leqslant j \leqslant c-1, \tag{A1}$$

$$\varphi_{1ij}(s) = \frac{\widehat{\mu}_i}{s+\lambda_i+\mu_i}\varphi_{1,i-1,j}(s) + \frac{\lambda_i}{s+\lambda_i+\mu_i}\varphi_{1,i+1,j}(s) + \frac{\widetilde{\mu}_i}{s+\lambda_i+\mu_i}\varphi_{0,i-1,j}(s), 1 \leqslant i \leqslant N, 1 \leqslant j \leqslant c-1. \tag{A2}$$

For any fixed $j \in \{0,\ldots,c-1\}$, Eq. (A1), for $1 \leqslant i \leqslant N-1$, can be expressed as

$$\beta_i^0\varphi_{0,i-1,j}(s) + \gamma_i^0\varphi_{0ij}(s) + \alpha_i^0\varphi_{0,i+1,j}(s) = \delta_i^0, \tag{A3}$$

where $\beta_1^0 = 0, \beta_i^0 = -\mu_i$, for $2 \leqslant i \leqslant N-2$, $\gamma_i^0 = s + \lambda_i + \mu_i$, for $1 \leqslant i \leqslant N-2, \alpha_i^0 = -\widehat{\lambda}_i$, for $1 \leqslant i \leqslant N-2$, and $\delta_i^0 = \widetilde{\lambda}_i \varphi_{1,i+1,j+1}(s)$, for $1 \leqslant i \leqslant N-2$.

Using a forward-elimination–backward-substitution (*FEBS*) procedure, the tridiagonal system of equations (A3) becomes

$$G_i^0 \varphi_{0ij}(s) + \alpha_i^0 \varphi_{0,i+1,j}(s) = D_i^0, \quad 1 \leqslant i \leqslant N-2, \tag{A4}$$

where $G_1^0 = \gamma_1^0 = s + \lambda_1 + \mu_1, G_i^0 = \gamma_i^0 - \beta_i^0 \alpha_{i-1}^0 / G_{i-1}^0 = s + \lambda_i + \mu_i - \mu_i \widehat{\lambda}_{i-1} / G_{i-1}^0$, for $2 \leqslant i \leqslant N-2, D_1^0 = \delta_1^0 = \widetilde{\lambda}_1 \varphi_{12,j+1}(s)$, and $D_i^0 = \delta_i^0 - \beta_i^0 D_{i-1}^0 / G_{i-1}^0 = \widetilde{\lambda}_i \varphi_{1,i+1,j+1}(s) + \mu_i D_{i-1}^0 / G_{i-1}^0$, for $2 \leqslant i \leqslant N-2$.

By defining $g_i^0 = G_i^0 - (s + \lambda_i)$, for $1 \leqslant i \leqslant N-2$, we avoid the use of negative terms that provide instability, and we reach the expressions for g_i^0 and D_i^0, for $1 \leqslant i \leqslant N-2$, appearing in Eqs. (5)–(8).

Next we use Eq. (A4) to express $\varphi_{0ij}(s)$ in terms of $\varphi_{0,i+1,j}(s)$

$$\varphi_{0ij}(s) = \frac{D_i^0 - \alpha_i^0 \varphi_{0,i+1,j}(s)}{G_i^0} = \frac{D_i^0 + \widehat{\lambda}_i \varphi_{0,i+1,j}(s)}{s + g_i^0 + \lambda_i}, \quad 1 \leqslant i \leqslant N-2. \tag{A5}$$

Iterating Eq. (A5) we get the expression in (2).

On the other hand, if we use the Eq. (A1) for $i = N-1$ and observe that $\widehat{\lambda}_{N-1} = 0$ and $\widetilde{\lambda}_{N-1} = \lambda_{N-1}$, then we obtain

$$(s + \lambda_{N-1} + \mu_{N-1}) \varphi_{0,N-1,j}(s) = \mu_{N-1} \varphi_{0,N-2,j}(s) + \lambda_{N-1} \varphi_{1N,j+1}(s). \tag{A6}$$

Now plugging Eq. (2) for $i = N-2$ in (A6), we get expression (1).

On the other side, transforms $\varphi_{1ij}(s)$, associated with states where the marked individual is infected, are manipulated in a similar way. First we fix the level $j \in \{1, \ldots, c-1\}$ and we express Eq. (A2), for $1 \leqslant i \leqslant N$, as follows:

$$\beta_i^1 \varphi_{1,i-1,j}(s) + \gamma_i^1 \varphi_{1ij}(s) + \alpha_i^1 \varphi_{1,i+1,j}(s) = \delta_i^1, \tag{A7}$$

where $\beta_1^1 = 0, \beta_i^1 = -\widehat{\mu}_i$, for $2 \leqslant i \leqslant N-1, \gamma_i^1 = s + \lambda_i + \mu_i$, for $1 \leqslant i \leqslant N-1$, $\alpha_i^1 = -\lambda_i$, for $1 \leqslant i \leqslant N-1$, and $\delta_i^1 = \widetilde{\mu}_i \varphi_{0,i-1,j}(s)$, for $1 \leqslant i \leqslant N-1$.

Once more, a *FEBS* method permits to express the tridiagonal system (A7) as

$$G_i^1 \varphi_{1ij}(s) + \alpha_i^1 \varphi_{1,i+1,j}(s) = D_i^1, \quad 1 \leqslant i \leqslant N-1, \tag{A8}$$

with $G_1^1 = \gamma_1^1 = s + \lambda_1 + \mu_1, G_i^1 = \gamma_i^1 - \beta_i^1 \alpha_{i-1}^1 / G_{i-1}^1 = s + \lambda_i + \mu_i - \widehat{\mu}_i \lambda_{i-1} / G_{i-1}^1$, for $2 \leqslant i \leqslant N-1, D_1^1 = \delta_1^1 = 0$, and $D_i^1 = \delta_i^1 - \beta_i^1 D_{i-1}^1 / G_{i-1}^1 = \widetilde{\mu}_i \varphi_{0,i-1,j}(s) + \widehat{\mu}_i D_{i-1}^1 / G_{i-1}^1$, for $2 \leqslant i \leqslant N-1$.

Again we avoid negative terms by introducing $g_i^1 = G_i^1 - (s + \lambda_i)$, for $1 \leqslant i \leqslant N-1$. Then, we get the coefficients appearing in Eqs. (9)–(12).

Using Eq. (A8) it is possible to express $\varphi_{1ij}(s)$ in terms of $\varphi_{1,i+1,j}(s)$ as follows:

$$\varphi_{1ij}(s) = \frac{D_i^1 - \alpha_i^1 \varphi_{1,i+1,j}(s)}{G_i^1} = \frac{D_i^1 + \lambda_i \varphi_{1,i+1,j}(s)}{s + g_i^1 + \lambda_i}, \quad 1 \leqslant i \leqslant N-1. \tag{A9}$$

Iterating Eq. (A9) we obtain Eq. (4).

Finally, Eq. (3) is determined by combining Eq. (A2), for $i = N$, and Eq. (4), for $i = N-1$. □

Appendix B. The number of infections per individual in an SIS model: Algorithmic schemes

Let the blocks $\mathbf{Q}_{ij}$ be as defined in Section 2.3. Now we introduce new auxiliary blocks $\mathbf{A}_i = \mathbf{Q}_{i,i-1}$, for $1 \leqslant i \leqslant N, \mathbf{B}_i = -\mathbf{Q}_{ii}$, for $1 \leqslant i \leqslant N-1, \mathbf{B}_N = \mu_N$, and

$$\mathbf{C}_i(z) = \begin{pmatrix} \widehat{\lambda}_i & z\widetilde{\lambda}_i \\ 0 & \lambda_i \end{pmatrix}, \quad 1 \leqslant i \leqslant N-2, \quad \mathbf{C}_{N-1}(z) = \begin{pmatrix} z\lambda_{N-1} \\ \lambda_{N-1} \end{pmatrix}, \quad \text{for } |z| \leqslant 1,$$

where the multiplicative factor z arising in the blocks $\mathbf{C}_i(z)$ is inherent to the infections assigned to the marked individual. We notice that $\psi_{00}(z) = 1$, and define $\psi_i(z) = (\psi_{0i}(z), \psi_{1i}(z))'$, for $1 \leqslant i \leqslant N-1$, and $\psi_N(z) = \psi_{1N}(z)$.

In this way, we present the following algorithm for the recursive computation of the generating functions $\psi_{ki}(z)$.

Algorithm 1

Step 1. Set $\mathbf{G}_1(z) = \mathbf{B}_1$.
Step 2. For $i = 2, \ldots, N$ do $\mathbf{G}_i(z) = \mathbf{B}_i - \mathbf{A}_i \mathbf{G}_{i-1}^{-1}(z) \mathbf{C}_{i-1}(z)$.
Step 3. Set $\mathbf{w}_1(z) = \mathbf{G}_1^{-1}(z) \mathbf{A}_1$.
Step 4. For $i = 2, \ldots, N$ do $\mathbf{w}_i(z) = \mathbf{G}_i^{-1}(z) \mathbf{A}_i \mathbf{w}_{i-1}(z)$.
Step 5. Set $\psi_N(z) = \mathbf{w}_N(z)$.
Step 6. For $i = N-1, \ldots, 1$ do $\psi_i(z) = \mathbf{w}_i(z) + \mathbf{G}_i^{-1}(z) \mathbf{C}_i(z) \psi_{i+1}(z)$.

The matrices $\mathbf{G}_i(z)$, for $1 \leqslant i \leqslant N$, are M-matrices [25], so that their inverse $\mathbf{G}_i^{-1}(z)$ exist and have positive entries. As a result, Algorithm 1 gives a stable recursive scheme where only 2×2 blocks are involved in the algebraic calculations; indeed $\mathbf{G}_N(z)$ and $\mathbf{w}_N(z)$ are scalar quantities. This feature relaxes the algorithmic storage and avoids possible instability problems.

We notice that $M_{ki}^0 = \psi_{ki}(1) = 1$, for $(k,i) \in S$. Moreover, $M_{00}^n = 0$, for $n \geqslant 1$. The calculation of the moments $\mathbf{M}_i^n = (M_{0i}^n, M_{1i}^n)'$, for $1 \leqslant i \leqslant N-1$, and $\mathbf{M}_N^n = M_{1N}^n$, for $n \geqslant 1$, in terms of the moment of order $n-1$ can be performed in a similar manner. We need to introduce

$$\mathbf{C}_i = \mathbf{C}_i(1) = \mathbf{Q}_{i,i+1}, \quad 1 \leqslant i \leqslant N-1,$$

$$\mathbf{d}_i^n = \begin{pmatrix} \widetilde{\lambda}_i n M_{1,i+1}^{n-1} \\ 0 \end{pmatrix}, \quad 1 \leqslant i \leqslant N-1, \ \mathbf{d}_N^n = 0.$$

Then, the corresponding *FEBS* block algorithm for the factorial moments is as follows.

Algorithm 2

Step 1. Set $\mathbf{G}_1 = \mathbf{B}_1$.
Step 2. For $i = 2, \ldots, N$ do $\mathbf{G}_i = \mathbf{B}_i - \mathbf{A}_i \mathbf{G}_{i-1}^{-1} \mathbf{C}_{i-1}$.
Step 3. Set $\mathbf{w}_1^n = \mathbf{G}_1^{-1} \mathbf{d}_1^n$.
Step 4. For $i = 2, \ldots, N$ do $\mathbf{w}_i^n = \mathbf{G}_i^{-1} (\mathbf{d}_i^n + \mathbf{A}_i \mathbf{w}_{i-1}^n)$.
Step 5. Set $\mathbf{M}_N^n = \mathbf{w}_N^n$.
Step 6. For $i = N-1, \ldots, 1$ do $\mathbf{M}_i^n = \mathbf{w}_i^n + \mathbf{G}_i^{-1} \mathbf{C}_i \mathbf{M}_{i+1}^n$.

Appendix C. The time to reach a specific state for an SIR model: Algorithmic schemes

Let $\Phi_{ij}(s), \theta_{ij}$ and $\widetilde{m}_{ij}$ be as they were defined in Section 3.1. First we present the recursive scheme for the computation of the L_{ij} Laplace transforms: $\Phi_{ij}(s)$.

Algorithm 3

Step 1. Set $\Phi_{mn}(s) = 1$.
Step 2. For $i = m-1, m-2, \ldots, 0$ calculate

$$\Phi_{in}(s) = \frac{\mu_{i+1}}{s + \lambda_{i+1,n} + \mu_{i+1}} \Phi_{i+1,n}(s).$$

Step 3. For $k = 1$, calculate

3.a.

$$\Phi_{m+k,n-k}(s) = \frac{\lambda_{m+k-1,n-k+1}}{s + \lambda_{m+k-1,n-k+1} + \mu_{m+k-1}} \Phi_{m+k-1,n-k+1}(s).$$

3.b. For $i = m+k-1, m+k-2, \ldots, 2$ compute

$$\Phi_{i,n-k}(s) = \frac{\mu_{i+1}}{s + \lambda_{i+1,n-k} + \mu_{i+1}} \Phi_{i+1,n-k}(s) + \frac{\lambda_{i-1,n-k+1}}{s + \lambda_{i-1,n-k+1} + \mu_{i-1}} \Phi_{i-1,n-k+1}(s).$$

3.c For $i = 0, 1$ calculate

$$\Phi_{i,n-k}(s) = \frac{\mu_{i+1}}{s + \lambda_{i+1,n-k} + \mu_{i+1}} \Phi_{i+1,n-k}(s).$$

Step 4. Set $k = k+1$. If $k \leqslant n$ go to Step 3.a.

We notice that the above recursive scheme also provides the computation of the probabilities of visiting the state $(i,j) \in S$; that is, $\theta_{ij} = P\{L_{ij} < \infty\} = \Phi_{ij}(0), (i,j) \in S$. We also observe that $\widetilde{m}_{ij}^0 = \theta_{ij}$ and $\widetilde{m}_{mn}^0 = 1$. By differentiating equations for the Laplace transforms $\Phi_{ij}(s)$, we obtain the algorithm for the computation of the moments $\widetilde{m}_{ij}^k$, for $k \geqslant 1$.

Algorithm 4

Step 1. Set $\widetilde{m}_{mn}^{k}=0$.
Step 2. For $i=m-1,m-2,\ldots,0$ calculate

$$\widetilde{m}_{in}^{k}=\frac{\mu_{i+1}}{\lambda_{i+1,n}+\mu_{i+1}}\widetilde{m}_{i+1,n}^{k}+\frac{k}{\lambda_{i+1,n}+\mu_{i+1}}\widetilde{m}_{in}^{k-1}.$$

Step 3. For $l=1$, calculate
3.a.

$$\widetilde{m}_{m+l,n-l}^{k}=\frac{\lambda_{m+l-1,n-l+1}}{\lambda_{m+l-1,n-l+1}+\mu_{m+l-1}}\widetilde{m}_{m+l-1,n-l+1}^{k}+\frac{k}{\lambda_{m+l-1,n-l+1}+\mu_{m+l-1}}\widetilde{m}_{m+l,n-l}^{k-1}.$$

3.b. For $i=m+l-1,m+l-2,\ldots,2$ compute

$$\widetilde{m}_{i,n-l}^{k}=\frac{\mu_{i+1}}{\lambda_{i+1,n-l}+\mu_{i+1}}\sum_{p=0}^{k}\binom{k}{p}\widetilde{m}_{i+1,n-l}^{p}\frac{(k-p)!}{\left(\lambda_{i+1,n-l}+\mu_{i+1}\right)^{k-p}}+\frac{\lambda_{i-1,n-l+1}}{\lambda_{i-1,n-l+1}+\mu_{i-1}}\sum_{p=0}^{k}\binom{k}{p}\widetilde{m}_{i-1,n-l+1}^{p}\frac{(k-p)!}{\left(\lambda_{i-1,n-l+1}+\mu_{i-1}\right)^{k-p}}.$$

3.c For $i=0,1$ calculate

$$\widetilde{m}_{i,n-l}^{k}=\frac{\mu_{i+1}}{\lambda_{i+1,n-l}+\mu_{i+1}}\widetilde{m}_{i+1,n-l}^{k}+\frac{k}{\lambda_{i+1,n-l}+\mu_{i+1}}\widetilde{m}_{i,n-l}^{k-1}.$$

Step 4. Set $l=l+1$. If $l\leqslant n$ go to Step 3.a.

Appendix D. The time to reach a critical number of infections in an SIR model

Let us consider the absorption probabilities, Laplace transforms and moments of the random variable S_{ij} as they were introduced in Section 3.2.

Laplace transforms $\Psi_{ij}(s)$ can be computed in the natural order $n-h\leqslant j\leqslant n$ and $1\leqslant i\leqslant m+n-j$ from the following system of recursive equations:

$$\Psi_{ij}(s)=0,\quad (i,j)\in S_A, \tag{D1}$$

$$\Psi_{ij}(s)=1,\quad j=n-h,\quad 2\leqslant i\leqslant m+n-j, \tag{D2}$$

$$\Psi_{ij}(s)=\frac{\mu_i}{s+\lambda_{ij}+\mu_i}\Psi_{i-1,j}(s)+\frac{\lambda_{ij}}{s+\lambda_{ij}+\mu_i}\Psi_{i+1,j-1}(s),\quad n-h+1\leqslant j\leqslant n,\ 1\leqslant i\leqslant m+n-j. \tag{D3}$$

For the recursive computation of the moments we appeal to the equations:

$$\widehat{m}_{ij}^{0}=\Psi_{ij}(0)=\tau_{ij},\quad (i,j)\in S, \tag{D4}$$

$$\widehat{m}_{ij}^{k}=0,\quad (i,j)\in S_A,\ k\geqslant 1, \tag{D5}$$

$$\widehat{m}_{ij}^{k}=0,\quad j=n-h,\ 2\leqslant i\leqslant m+n-j,\ k\geqslant 1, \tag{D6}$$

$$\widehat{m}_{ij}^{k}=\frac{\mu_i}{\lambda_{ij}+\mu_i}\widehat{m}_{i-1,j}^{k}+\frac{\lambda_{ij}}{\lambda_{ij}+\mu_i}\widehat{m}_{i+1,j-1}^{k}+\frac{k}{\lambda_{ij}+\mu_i}\widehat{m}_{ij}^{k-1},\quad n-h+1\leqslant j\leqslant n,\ 1\leqslant i\leqslant m+n-j,\ k\geqslant 1. \tag{D7}$$

The Eqs. (D1)–(D3) follow from a first-step argument conditioning on the first transition out of a state $(i,j)\in S$. On the other hand, for $(i,j)\in S$, we observe that $\tau_{ij}=\Psi_{ij}(0)=\widehat{m}_{ij}^{0}$ so the absorption probabilities (D4), or order zero moments, are the solution of equations (D1)–(D3) for $s=0$. Eqs. (D5)–(D7) are obtained by differentiating Eqs. (D1)–(D3) k times with regard to s and setting $s=0$.

References

[1] H. Andersson, T. Britton, Stochastic epidemic models and their statistical analysis, Lecture Notes in Statistics, vol. 151, Springer, New York, 2000.
[2] J.R. Artalejo, A. Economou, M.J. Lopez-Herrero, On the number of recovered individuals in the SIS and SIR stochastic epidemic models, Math. Biosci. 228 (2010) 45–55.
[3] J.R. Artalejo, A. Economou, M.J. Lopez-Herrero, Stochastic epidemic models revisited: analysis of some continuous performance measures, J. Biol. Dyn. 6 (2012) 189–211.
[4] F. Chamchod, S. Ruan, Modeling the spread of methicillin-resistant staphylococcus aureus in nursing homes for elderly, PloS One 7 (2012). art. no. e29757.
[5] P. Stone, H. Wilkinson-Herbots, V. Isham, A stochastic model for head lice infections, J. Math. Biol. 56 (2008) 743–763.
[6] L.J.S. Allen, An introduction to stochastic epidemic models, Lecture Notes in Mathematics, vol. 1945, Springer, Berlin, 2008, pp. 81–130.
[7] T. Britton, Stochastic epidemic models: a survey, Math. Biosci. 225 (2010) 24–35.
[8] M.J. Keeling, J.V. Ross, On methods for studying stochastic disease dynamics, J.R. Soc. Interface 5 (2008) 171–181.
[9] D.J. Daley, J. Gani, Epidemic modelling: an introduction, Cambridge Studies in Mathematical Biology, vol. 15, Cambridge University Press, Cambridge, 1999.
[10] A. Gomez-Corral, M. Lopez-Garcia, Modeling host–parasitoid interactions with correlated events, Appl. Math. Model. 37 (2013) 5452–5463.
[11] S. Kondakci, C. Dincer, Internet epidemiology: healthy, susceptible, infected, quarantined, and recovered, Security Commun. Networks 4 (2011) 216–238.
[12] I. Nåsell, Extinction and quasi-stationarity in the stochastic logistic SIS model, Lecture Notes in Mathematics, vol. 2022, Springer, Berlin, 2011.
[13] H. Okamura, H. Kobayashi, T. Dohi, Markovian modeling and analysis of Internet worm propagation, in: Proceedings of the 16th IEEE International Symposium on Software, Reliability Engineering, 2005, pp. 149–158.
[14] Y. Wang, C. Lin, Q.L. Li, Performance analysis of email systems under three types of attacks, Perform. Eval. 67 (2010) 485–499.
[15] J.C. Wierman, D.J. Marchette, Modeling computer virus prevalence with a susceptible-infected-susceptible model with reintroduction, Comput. Stat. Data Anal. 45 (2004) 3–23.
[16] J.R. Artalejo, M.J. Lopez-Herrero, On the exact measure of disease spread in stochastic epidemic models, Bull. Math. Biol. 75 (2013) 1031–1050.
[17] J.V. Ross, Invasion of infectious diseases in finite homogeneous populations, J. Theor. Biol. 289 (2011) 83–89.
[18] J.R. Artalejo, M.J. Lopez-Herrero, Quasi-stationarity and ratio of expectations distributions: a comparative study, J. Theor. Biol. 266 (2010) 264–274.
[19] I. Nåsell, Extinction and quasi-stationarity in the Verhulst logistic model, J. Theor. Biol. 211 (2001) 11–27.
[20] E.A. van Doorn, P.K. Pollett, Survival in a quasi-death process, Linear Algebra Appl. 429 (2008) 776–791.
[21] T. House, J.V. Ross, D. Sirl, How big is an outbreak likely to be? Methods for epidemic final-size calculation, Proc. R. Soc. A 469 (2013). no. 2150.
[22] J. Abate, W. Whitt, Numerical inversion of Laplace transforms of probability distribution, ORSA J. Comput. 7 (1995) 36–43.
[23] A.M. Cohen, Numerical Methods for Laplace Transform Inversion, Springer, New York, 2007.
[24] H.C. Tijms, A First Course in Stochastic Models, Wiley, Chichester, 2003.
[25] P.G. Ciarlet, Introduction to Numerical Linear Algebra and Optimization, Cambridge University Press, Cambridge, 1989.
[26] R. Bhattacharyya, B. Mukhopadhyay, On a epidemiological model with nonlinear infection incidence: local and global perspective, Appl. Math. Model. 35 (2011) 3166–3174.
[27] N.C. Severo, Generalizations of some stochastic epidemic models, Math. Biosci. 4 (1969) 395–402.
[28] M.F. Neuts, J.-M. Li, An algorithmic study of S-I-R Stochastic epidemic models, in: C.C. Heyde, Yu V. Prohorov, R. Pyke, S.T. Rachev (Eds.), Athens Conference on Applied Probability and Time Series, vol. 1, Springer-Verlag, Heidelberg, 1996, pp. 295–306.
[29] R.P. Wenzel, A.A. Fowler III, M.B. Edmond, Antibiotic prevention of acute exacerbations of COPD, N. Engl. J. Med. 367 (2012) 340–347.
[30] J.C. Nickel, Practical management of recurrent urinary tract infections in premenopausal women, Rev. Urol. 7 (2005) 11–17.
[31] J.R. Artalejo, M.J. Lopez-Herrero, The SIS and SIR stochastic epidemic models: a maximum entropy approach, Theor. Popul. Biol. 80 (2011) 256–264.
[32] J.V. Ross, D.E. Pagendam, P.K. Pollett, On parameter estimation in population models II: multi-dimensional processes and transient dynamics, Theor. Popul. Biol. 75 (2009) 123–132.
[33] N. Bacaër, M.G.M. Gomes, On the final size of epidemics with seasonality, Bull. Math. Biol. 71 (2009) 1954–1966.
[34] N. Bacaër, M. Khaladi, On the basic reproduction number in a random environment, J. Math. Biol. (2013), http://dx.doi.org/10.1007/s00285-012-0611-0.
[35] A. Gray, D. Greenholgh, X. Mao, J. Pan, The SIS epidemic model with Markovian switching, J. Math. Anal. Appl. 394 (2012) 496–516.